Supporting Information

Dumbbell-Shaped Nanorods Assembly of NiO/CuO Composite for High-Performance Redox-Active Battery-Type Supercapacitor Electrodes

Mulla Jakeer Hussain[a], Mohamed A. Ghanem[b], Y. Veera Manohara Reddy[c], G. Madhavi[a*], Sang Woo Joo[d*], and Gutturu Rajasekhara Reddy[d*]

[a]*Department of Chemistry, Sri Venkateswara University, Tirupati, 516380, India*

[b]*Chemistry Department, College of Science, King Saud University, Riyadh, 11451, Saudi Arabia*

[c]*Department of Chemistry, Sri Venkateswara College (University of Delhi), New Delhi 110021, India*

[d]*School of Mechanical Engineering, Yeungnam University, Gyeongsan 38541, Republic of Korea*

*Corresponding author's email: gmchem01@gmail.com

swjoo@yu.ac.kr

gutturur ajasekharareddy@gmail.com

1. Experimental section

1.1 Chemicals and materials

All the analytical reagent-grade chemicals were used as received, without purification. Nickel(II) nitrate hexahydrate ($Ni(NO_3)_2{\cdot}6H_2O$; ≥99), Copper(II) nitrate trihydrate ($Cu(NO_3)_2{\cdot}3\ H_2O$; ≥ 98%), urea (CO(NH2)2; 99.0-100.5%), poly(vinylidene fluoride) (PVDF; average Mw ~534,000 by GPC), N-methyl-2-pyrrolidone (NMP; ≥ 99%), and potassium hydroxide (KOH; ≥99.95% trace metals basis) were purchased from Sigma–Aldrich MeRCK, Seoul, South Korea. Ethanol

(DUKSAN Reagents and Chemicals, extra pure 99.9%). Nickel foam (MTI Korea, Seoul, South Korea, 99.95%), HCl (Sigma Aldrich MeRCK, ACS reagents, Seoul, South Korea, 37%), acetone (DUKSAN Reagents and Chemicals, Gyeonggi-do, Gyeonggi-do, South Korea, extra pure 99.9%), carbon black (DENKA BLACK, Highly purified and extremely conductive acetylene black, Kyoto, Japan).

1.2 Physicochemical CuO/NiO composite characterizations

The crystallinity and phase formation of the pristine NiO and NiO/CuO composite samples were investigated using an X-ray diffractometer (PANanalytical X-Pert Pro) operating at 40 kV and 30 mA with Cu Kα radiation (λ = 1.540 Å). The sample surface morphologies were examined using field-emission scanning electron microscopy (FESEM, S-4800, Hitachi, Japan), while elemental mapping was conducted via an X-ray column integrated with the FESEM system. High-resolution transmission electron microscopy (HRTEM, Tecnai G2 F20 S-Twin, USA) was performed for NiO/CuO Composite. The chemical composition and oxidation states of the samples were characterized by X-ray photoelectron spectroscopy (XPS, K-alpha, Thermo Scientific, USA) and the data were processed using Thermo Scientifics Avantage software (version 5.932). Nitrogen adsorption–desorption isotherms of pristine NiO and NiO/CuO composite were obtained using a 3-Flex surface analyzer (Micromeritics, USA).

1.3 Electrode preparation

Nickel (Ni) foam was used as the current collector for the deposition of the active electrode material. Before applying the working electrode to a 2.5 × 1 cm^2 piece of Ni foam, the foam underwent a thorough cleaning procedure via ultrasonication in 1 M hydrochloric acid (HCl), deionized water, and absolute ethanol for 5 minutes each to remove any surface oxide layers.

Following this, the foam was dried at 70 °C for overnight. A mixture of the synthesized active materials, polyvinylidene fluoride (PVDF) as a binder, and carbon black to enhance conductivity, was prepared in a weight ratio of 80:10:10. This blend was then dispersed in 0.5 mL of N-methyl-2-pyrrolidone (NMP). The resulting slurry was drop-cast evenly onto the pre-cleaned Ni foam, covering an area of 1.5 × 1 cm², and left to dry at 80 °C overnight. Finally, a pressure of 10 MPa was applied to ensure a uniform thin film of the active material. The mass loading of the electrode material was approximately 3.5 mg, optimizing it for electrochemical performance comparison.

1.4 Electrochemical characterization

All electrochemical tests were performed at room temperature using a Bio-Logic electrochemical workstation equipped with EC-Lab software (version V11.36). The electrochemical setup comprised a Hg/HgO reference electrode, a platinum mesh counter electrode, and nickel foam coated with the active material as the working electrode. A 6 M KOH aqueous solution was used as the electrolyte. To assess the electrochemical properties of the synthesized samples, cyclic voltammetry (CV), galvanostatic charge-discharge (GCD), and electrochemical impedance spectroscopy (EIS) measurements were carried out. The specific capacity (C_s; C g^{-1}) of the electrodes was calculated using the equation:

$$C_s = \frac{I\Delta t}{m} \text{ C g}^{-1}$$

In this equation, I (A g^{-1}) denotes the applied current density, Δt(s) indicates the discharge time, and m(g) represents the mass of the active electrode materials.

2. Results and discussion

Pure CuO was synthesized following the same procedure used for NiO, with $Ni(NO_3)_2 \cdot 6H_2O$ replaced by $Cu(NO_3)_2 \cdot 3H_2O$. The obtained sample was characterized using XRD, and the corresponding diffraction pattern is presented in **Figure S2**. The XRD pattern displays characteristic peaks at 2θ values of 32.60, 35.51, 38.74, 46.33, 48.85, 53.61, 58.42, 61.44, 66.38, and 68.14°, which are indexed to the (110), (−111), (200), (−112), (−202), (020), (202), (−113), (−311), and (220) planes, respectively, of monoclinic CuO (JCPDS card no. 00-041-0254, space group C2/c). This confirms the successful formation of phase-pure CuO. Additionally, few peaks observed at 36.48° and 42.35°, corresponding to the (111) and (200) planes of cubic Cu_2O (JCPDS card no. 01-078-2076, space group Pn-3m), indicate the presence of a secondary Cu_2O phase, resulting in a CuO/Cu_2O composite.

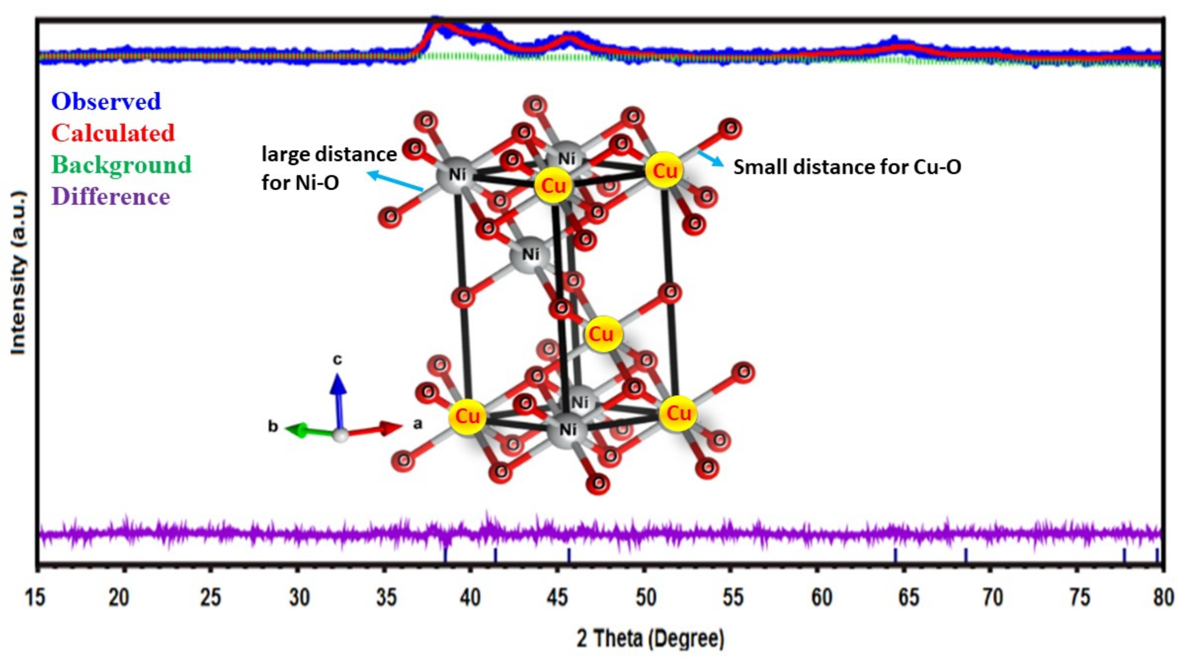

Figure S1. Rietveld refinement of the XRD spectra for the NiO/CuO composite. The inset of structural diagrams was generated using the refinement parameters provided in **Table 1**. In the ball-and-stick model, the gray, red and orange spheres represent Ni and O atoms, respectively.

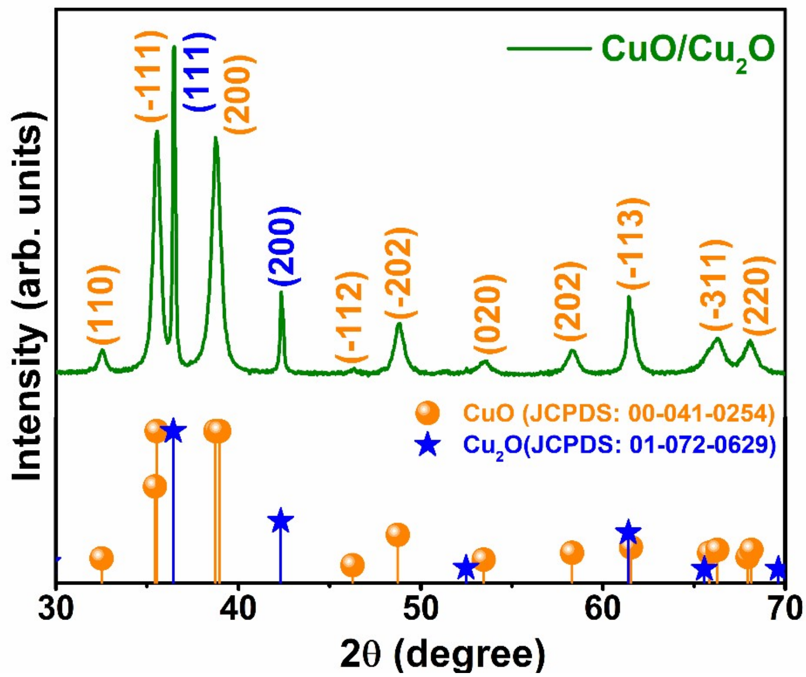

Figure S2. XRD pattern of the as-synthesized CuO/Cu_2O sample.

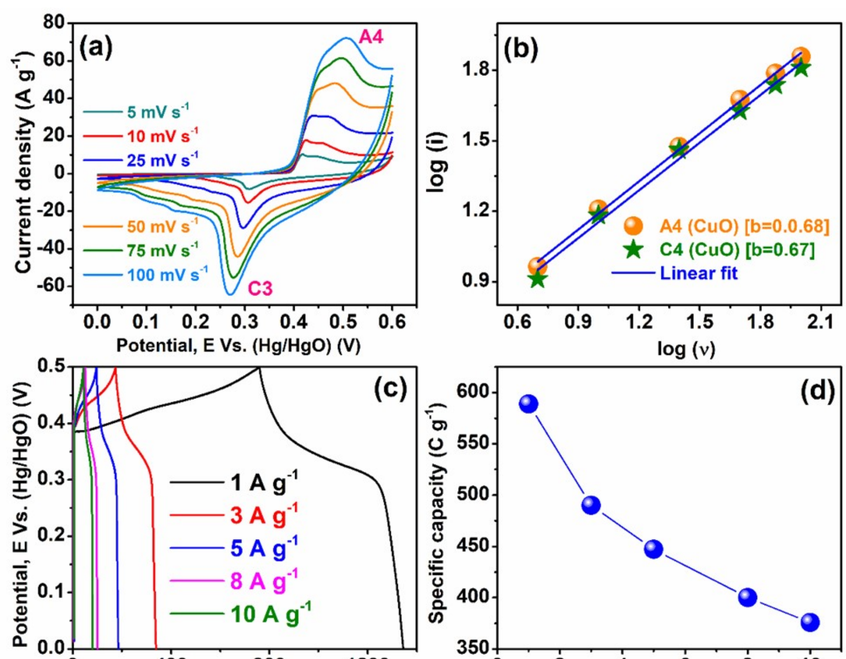

Figure S3. Electrochemical performance of the CuO/Cu_2O electrode: (a) CV curves at various scan rates, (b) log(i) vs. log(v) plot, (c) GCD curves at different current densities, and (d) specific capacity as a function of current density.